

Theory of quantum backaction enhancement and displacement measurement using a multiple cavity mode transducer

J. M. Dobrindt¹ and T.J. Kippenberg^{1,2,*}

¹Max Planck Institut für Quantenoptik, D-85748 Garching, Germany

²Ecole Polytechnique Fédérale de Lausanne (EPFL), CH-1015 Lausanne, Switzerland

A readout scheme for achieving quantum limited displacement sensing of high frequency mechanical oscillator is presented, whose frequency greatly exceeds the cavity decay rate used for parametric motion transduction. The coupling of a mechanical degree of freedom to several optical modes spaced by the mechanical oscillator frequency allows substantial reduction of the power required to reach the standard quantum limit, compared to the case of coupling to a single cavity resonance. Moreover, quantum back-action is enhanced in this scheme, relevant across a wide range of quantum-optomechanical experiments. Straightforward implementation of the scheme in both microwave and optical domain is discussed.

PACS numbers: 42.60.Da, 42.81.Qb

Introduction.— The measurement of mechanical displacement using a parametric cavity transducer[1] is pivotal in a wide range of studies covering fundamental science and technology, and is of major concern in gravitational wave detection[2]. The canonical system that is used to describe a parametric motion transducer is an optical cavity with a movable mirror[3]. Ideally, under condition of continuous detection of motion, the displacement sensitivity is limited by the standard quantum limit (SQL). The SQL pertains to the minimum uncertainty in motion detection and arises from the trade off between measurement imprecision, inherent to the meter (i.e., detector shot noise), and (for linear continuous measurements) inevitable *quantum backaction* (QBA)[4, 5]. These two noise processes are characterized by the displacement spectral density $\bar{S}_{xx}[\Omega]$ and the radiation pressure force spectral density $\bar{S}_{FF}[\Omega]$ [27].

$$\bar{S}_{xx}[\Omega] = \frac{x_0^2 \kappa}{4g_m^2} \left[1 + \frac{4\Omega^2}{\kappa^2} \right]; \quad \bar{S}_{FF}[\Omega] = \frac{\hbar^2 g_m^2}{x_0^2 \kappa} \left[1 + \frac{4\Omega^2}{\kappa^2} \right]^{-1} \quad (1)$$

Here, g_m is the optomechanical coupling rate, κ is the cavity decay rate, and $x_0 = \sqrt{\hbar/2m_{eff}\Omega_m}$ denotes the zero point fluctuation of the mechanical oscillator (characterized by its effective mass m_{eff} and mechanical frequency Ω_m). Note that $g_m^2 \propto P/\kappa$ where P is the launched input power. The existence of the SQL can equally be viewed as a manifestation of the Heisenberg uncertainty principle[1], $\sqrt{S_{xx}[\Omega]S_{FF}[\Omega]} \geq \hbar/2$. It is noteworthy, that QBA, while predicted by Caves two decades ago[6], has never been observed experimentally in the context of mechanical displacement measurements[7]. Recently, experiments employing nanomechanical oscillators coupled to a SET[8], LC circuit[9], superconducting microwave resonator[10] or cavity optomechanical systems[11, 12], have made significant progress in approaching the SQL and observing QBA. Here, we introduce a measurement scheme, where both, QBA and sensitivity of the meter, are enhanced for

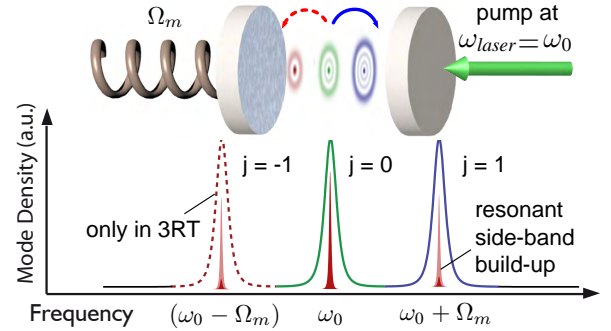


Figure 1: In a cavity with a harmonically bound end mirror and three (two) optical modes spaced by the mechanical resonant frequency, sideband build-up at $\omega_0 (\mp) \Omega_m$ is enhanced.

a given input power, and thus the SQL and the QBA-dominated regime are attained at significantly lower input power. Equations 1 show, that the power where the SQL is reached (P_{SQL}), decreases, when lowering the cavity decay rate of the transducer (κ). Experimentally this is highly desirable, as high input power usually entails parasitic sources of noise, e.g. cavity heat-up and non-linearity. However, Eqs. 1 reveals a fundamental deficiency: decreasing the decay rate of the cavity for fixed input power (P) and mechanical frequency (Ω_m), improves readout sensitivity as long as $\kappa > \Omega_m$, while for $\kappa < \Omega_m$ the displacement sensitivity experiences saturation. Physically this phenomenon is readily understood; the mechanical motion modulates the cavity field and creates sidebands at $\omega \pm \Omega_m$, which constitute the readout signal. For $\kappa \ll \Omega_m$, i.e., in the resolved sideband regime (RSB), the sidebands (and therefore the signal) are suppressed, as they are not resonant [cf. Fig. 1]. The RSB has recently been subject to experimental investigation [10, 13], as it is prerequisite to ground state cooling[14, 15].

Here, we present a novel readout scheme which solves this

deficiency by using multiple cavity resonances. Explicitly we discuss [cf. Fig.1]: i) a *three resonance scheme* (3RT) with two secondary resonances placed at $\omega_0 \pm \Omega_m$. This entails efficient sideband build-up, leading to a stronger signal at $\pm\Omega_m$; ii) a *two resonance scheme* (2RT) with one auxiliary resonance at $\omega_0 + \Omega_m$. The 3RT will be compared to the resonant single mode transducer (1RT, only $j = 0$ mode), while the 2RT is reminiscent of the red detuned single mode transducer (1RT_{det}, only $j = 1$ mode). In the latter, as in the 2RT, asymmetric sideband build-up (the Anti-Stokes process has higher probability than the Stokes process) entails cooling of the mechanical oscillator[14, 15]. Moreover, we demonstrate that the 2RT and 3RT substantially lower the power, required to reach the QBA-dominated regime. Achieving this regime is of interest in a variety of quantum optomechanical experiments, such as radiation pressure squeezing or two mode squeezing[7].

Theoretical model.— Starting point of the analysis is a cavity optomechanical setting, constituted by a Fabry-Pérot type cavity with a harmonically bound back mirror. A driving field s_+ at frequency ω_0 (with input power $P = |s_+|^2$) is coupled (input coupling rate κ_{ex}) to a resonant cavity mode. Cavity loss is modeled by a vacuum port (coupling rate κ_{in}), and the total cavity decay rate is $\kappa = \kappa_{ex} + \kappa_{in}$. Here we define the coupling parameter $\eta_c = \kappa_{ex}/\kappa$. The dual scheme is modeled by introducing an additional, blue-detuned, optical mode at frequency $\omega_0 + \Omega_m$, and the triple scheme by adding yet another optical mode at $\omega_0 - \Omega_m$. The modes are addressed by the index j , referring to their resonant frequency $\omega_0 + j\Omega_m$ [cf. Fig1], and are described by the annihilation(creation) operators \hat{a}_j (\hat{a}_j^\dagger). The modes parametrically interact with the mechanical oscillator, via the interaction Hamiltonian [28]

$$\hat{H}_{int} = \sum_{i,j=0,1,(-1)} \hbar\eta\Omega_m \hat{a}_i^\dagger \hat{a}_j (\hat{a}_m + \hat{a}_m^\dagger). \quad (2)$$

The optomechanical coupling strength is expressed by the cavity frequency shift due to mirror displacement $\eta = (x_0/\Omega_m) \frac{d\omega_0}{dx}$. In the next step, we introduce the general quadrature $\hat{X}_{j,\Theta} = e^{-i\Theta}\hat{a}_j + e^{i\Theta}\hat{a}_j^\dagger$ and derive the Heisenberg-Langevin equations for the canonical quadratures $\hat{X}_j = \hat{X}_{j,\Theta=0}$ and $\hat{Y}_j = \hat{X}_{j,\Theta=\pi/2}$. Noise, originating from intrinsic and coupling loss, is introduced in the usual way[16]. Subsequently the coherent driving term ($\propto s_+$) is eliminated by transformation to a rotating frame and shifting the operators to their steady states ($\hat{a}_j \rightarrow \bar{a}_j + \hat{a}_j$). The global phase is chosen in the way that $\bar{a} = \Sigma \bar{a}_j$ (\bar{a}_j : steady state of a_j) is real[29]. Then the optomechanical coupling rate $g_m = 2\eta\Omega_m\bar{a}$ is real

and the linearized Heisenberg-Langevin equations are

$$\begin{aligned} \dot{\hat{X}}_j &= \Delta_j \hat{Y}_j - \frac{\kappa}{2} \hat{X}_j + \frac{g_m^2}{4\Omega_m} \left(\sum_k \hat{Y}_k - \delta_{kj} \hat{Y}_j \right) \\ &\quad + \sqrt{\kappa_{ex}} \delta \hat{X}_j^{in}(t) + \sqrt{\kappa_{in}} \delta \hat{X}_j^{vac}(t) \\ \dot{\hat{Y}}_j &= -\Delta_j \hat{X}_j - \frac{\kappa}{2} \hat{Y}_j - \frac{g_m^2}{4\Omega_m} \left(\sum_k \hat{X}_k - \delta_{kj} \hat{X}_j \right) \\ &\quad + g_m \hat{Q}(t) + \sqrt{\kappa_{ex}} \delta \hat{Y}_j^{in}(t) + \sqrt{\kappa_{in}} \delta \hat{Y}_j^{vac}(t). \end{aligned} \quad (3)$$

The noise operators are assumed to be δ -correlated: $\langle \delta \hat{X}_i^{in}[t] \delta \hat{X}_j^{in}[t'] \rangle = \langle \delta \hat{Y}_i^{in}[t] \delta \hat{Y}_j^{in}[t'] \rangle = \delta_{ij} \delta(t-t')$, $\langle \delta \hat{X}_i^{in}[t] \delta \hat{Y}_j^{in}[t'] \rangle = \langle \delta \hat{Y}_i^{in}[t] \delta \hat{X}_j^{in}[t'] \rangle^* = i\delta_{ij} \delta(t-t')$. The same relations apply to the noise entering through the vacuum port ($\delta \hat{X}_j^{vac}, \delta \hat{Y}_j^{vac}$). Here, we neglect the field-field coupling ($\propto g_m^2$) in Eqs. 3. The additional terms only become important, when the system is already dominated by quantum backaction and are, therefore, not of interest in the present discussion. Introducing the $2N \times 1$ vectors $\vec{X} = (\hat{X}_1, \hat{Y}_1, \dots, \hat{X}_N, \hat{Y}_N)^\top$ (and, correspondingly, the noise vectors $\delta \vec{X}^{in}$ and $\delta \vec{X}^{vac}$, as well as the auxiliary vector $\vec{T}_\Theta = (\cos \Theta, \sin \Theta, \dots, \cos \Theta, \sin \Theta)^\top$), we transform Eqs. 3 to Fourier space to eliminate the time derivatives and solve for $\vec{X}[\Omega] = \tilde{\mathbf{M}}[\Omega] \left(g_m Q[\Omega] \vec{T}_{\pi/2} + \sqrt{\kappa_{ex}} \delta \vec{X}^{in}[\Omega] + \sqrt{\kappa_{in}} \delta \vec{X}^{vac}[\Omega] \right)$.

Here, the matrix $\tilde{\mathbf{M}}[\Omega]$ is implicitly defined by the Eqs. 3 and does not contain any properties of the mechanical mode. The signal $Q[\Omega]$ is introduced and coupled into the phase quadrature (\hat{Y}_j) to derive the transduction function of the cavity[17].

Displacement sensitivity.— In the first place we calculate the generalized output quadrature using the input-output formalism [16]. It is important to emphasize, that considering the input fluctuations at the cavity port is necessary in the RSB, in contrast to the Doppler regime ($\kappa \gg \Omega_m$), where they can be neglected[18]. For multiple cavity modes the output quadrature fluctuations are given by $X_\Theta^{out}[\Omega] = (1/\sqrt{N}) \sum_j (\sqrt{\kappa_{ex}} X_{j,\Theta}[\Omega] + X_{j,\Theta}^{in}[\Omega])$, with N being the number of optical modes. Here we solve the full system, including the mechanical degree of freedom. The corresponding output quadrature can be decomposed into the following form:

$$\hat{X}_\Theta^{out}[\Omega] = \hat{I}_x[\Omega] + \hat{I}_F[\Omega] + \lambda(\Omega) \tilde{Q}[\Omega] \quad (4)$$

For the 1RT this reproduces the result of Ref.[19]; yet, here, the terms are separated by their physical origin[17, 20]. The first term gives rise to the detector shot noise background with $\langle \hat{I}_x[\Omega] \hat{I}_x[\Omega'] \rangle = 2\pi\delta(\Omega + \Omega')$.

The second term, \hat{I}_F , is the response of the mechanical oscillator to vacuum field fluctuation (i.e., quantum backaction). It vanishes when the effective mass

of the mirror is taken to infinity, while the detection noise $\hat{I}_x[\Omega]$ remains unaffected by this operation. In the same sense, the transduction function $\lambda(\Omega) = \sqrt{\eta_c \kappa / N} (g_m / x_0) \left\{ \tilde{T}_\Theta^\dagger \tilde{\mathbf{M}}[\Omega] \tilde{T}_{\pi/2} \right\}$ is a pure cavity property, and the dynamical backaction[21] of the mechanics is contained in the effective susceptibility $\chi_{eff}(\Omega)$, which is defined by the effective length change of the cavity $\tilde{Q}[\Omega] = \{\chi_{eff}(\Omega) / \chi_0(\Omega)\} Q[\Omega]$ in response to the displacement signal $Q[\Omega]$. The properties of the mechanics only enter via the effective susceptibility and the definition of \hat{I}_F . We note, that for the detuned 1RT_{det} and 2RT in the RSB, the signal is suppressed and modified by dynamic backaction effects and is furthermore complicated by correlations between \hat{I}_x and \hat{I}_F . These correlations, usually expressed by the spectral density $S_{xF}[\Omega]$, entail squeezing[19, 22] and will not be discussed here. In contrast, for the resonant 1RT and the 3RT, there are no dynamic backaction effects, i.e., $\chi_{eff}(\Omega) = \chi_0(\Omega)$ [23]. Here we scale the measurement uncertainty to the effective signal, so that the symmetrized spectral density $\bar{S}_{xx}[\Omega] = |\lambda(\Omega)|^{-2}$, and we denote $|\lambda(\Omega)|^2$ the sensitivity of the meter. Comparing the 2RT and 3RT to the resonant 1RT in Fig. 2, the sensitivity at the mechanical resonance frequency ($\Omega = \Omega_m$) is increased by, respectively, $1/8 \times 4\Omega_m^2 / \kappa^2$ and $1/3 \times 4\Omega_m^2 / \kappa^2$. Note that for the 2RT (and also for the detuned 1RT_{det}) the signal at Ω_m is imprinted in *both* quadratures of the output field, which is visualized in Fig. 2 and will later re-appear in the uncertainty product of the general 1RT (Eq.7).

Backaction force spectral density.— From Eq. 4 we calculate the backaction force spectral density via the relation $2\pi\delta(\Omega + \Omega') S_{FF}[\Omega] = \langle \hat{I}_F[\Omega] \hat{I}_F[\Omega'] \rangle / |\lambda(\Omega) \chi_{eff}(\Omega)|^2$. When neglecting the field-field interaction in Eq. 3, the backaction force spectral density can be written as the sum of spectral densities $S_{FF} = \sum_{j=0,1,(-1)} S_{FF,j}$, which originate from the single optical resonances

$$S_{FF,j}[\Omega] = g_m^2 \frac{\hbar^2}{x_0^2} \frac{\kappa}{\kappa^2/4 + (\Omega - j\Omega_m)^2} \quad (5)$$

The dominant contribution to the backaction force comes from the resonance that is blue detuned (index $j = 1$) from the driving field[15]. Comparing the 3RT to the 1RT, this particular resonance leads to a large increase in QBA, that is well estimated by $S_{FF}^{triple}[\Omega_m] / S_{FF}^{single}[\Omega_m] \approx 4\Omega_m^2 / \kappa^2$ [cf. Fig.3]. In the RSB ($\kappa \ll \Omega_m$), this easily enhances QBA by a few orders of magnitude[10, 13]. Compared to the 1RT_{det}, the QBA in the 2RT is barely increased for the same intracavity power ($\propto g_m^2$)[30], as $(S_{FF,0}[+\Omega_m] \ll S_{FF,1}[+\Omega_m])$ [15]. Yet the probability of a Stokes process, transferring energy from the cavity (rotating frame) to the mechanical mode changes, because $S_{FF,0}[-\Omega_m] \approx 4 \cdot S_{FF,1}[-\Omega_m]$, which directly affects the final occupancy of the mechanical mode, that can be reached in backaction cooling.

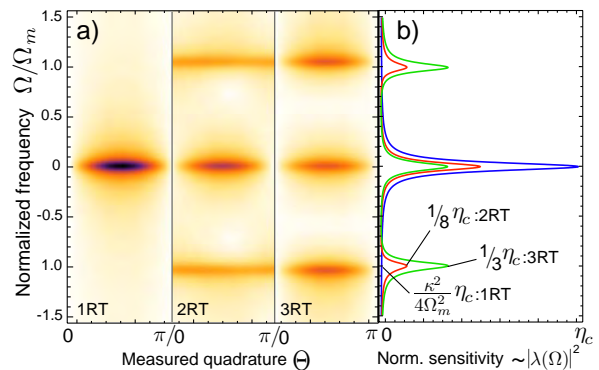


Figure 2: [for $\kappa = \Omega_m/10$] (a) The normalized sensitivity $|\lambda(\Omega)|^2$ is shown as a function of Ω and Θ . The scale is given by the cross sections at $\Theta = \pi/2$ in panel (b). For the 2RT and 3RT the sensitivity at $\Omega = \Omega_m$ is increased towards the 1RT by, respectively, $1/8 \times (4\Omega_m^2 / \kappa^2)$ and $1/3 \times (4\Omega_m^2 / \kappa^2)$. Note, that for the 2RT, the signal at Ω_m is coupled to both quadratures (amplitude and phase). For $\kappa \ll \Omega_m$, the integral of $|\lambda|^2$ over Θ and Ω is the same for all three cases.

Compared to the single resonance dynamic backaction cooling[14, 15], the quantum limit increases by a factor of $\times 5$.

$$\frac{n_f + 1}{n_f} = \frac{S_{FF}^{dual}[+\Omega_m]}{S_{FF}^{dual}[-\Omega_m]}, \Rightarrow n_f \approx 5 \frac{\kappa^2}{16\Omega_m^2} \quad (6)$$

Standard quantum limit.— Quantum measurement theory predicts, that a displacement measurement is bound by the Heisenberg uncertainty principle[1]. This entails that $\sqrt{S_{xx}[\Omega_m] \cdot S_{FF}[\Omega_m]} = \hbar/2$ for the well studied resonant 1RT (in the limit of overcoupling, i.e., $\eta_c \rightarrow 1$). Introducing an arbitrary detuning $\Delta = \omega_{laser} - \omega_0$ in the 1RT, we calculate the uncertainty products for the general 1RT and 3RT. Symmetrizing the expressions for S_{xx} and S_{FF} , the SQL is formulated when minimizing the product with respect to the quadrature angle Θ .

$$\begin{aligned} \bar{S}_{xx}^{single}[\Omega] \cdot \bar{S}_{FF}^{single}[\Omega] &\geq \\ &\frac{\hbar^2}{4\eta_c} \frac{2}{1 + \sqrt{1 - 4\Delta^2\Omega^2 / (\Delta^2 + \frac{\kappa^2}{4} + \Omega^2)}} \\ \bar{S}_{xx}^{triple}[\Omega] \cdot \bar{S}_{FF}^{triple}[\Omega] &\geq \\ &\frac{\hbar^2}{4\eta_c} \sqrt{1 + 2 \frac{64\Omega_m^4 + 12\Omega_m^2\kappa^2}{64\Omega_m^4 + 96\kappa^2\Omega_m^2 + 9\kappa^4}} \end{aligned} \quad (7)$$

In both cases, for the optimal measured quadrature ($\Theta \rightarrow \Theta_{opt}$), the \geq sign becomes an equal sign. The expression for the 1RT shows clearly, that in the parameter regime $\kappa \ll \Delta \approx \Omega_m$, relevant for RSB ground state cooling, the SQL is missed by a factor of two. Analogous to the 2RT, the signal is transduced in both quadratures, while only one is recorded. However the uncertainty product does, in general, not correspond to the overall measurement

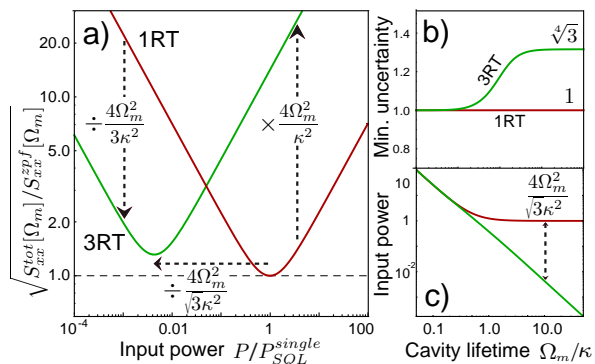


Figure 3: (a) The (normalized) measurement uncertainty $S_{xx}^{tot}[\Omega_m] = S_{xx}[\Omega_m] + |\chi_{eff}[\Omega_m]|^2 S_{FF}[\Omega_m]$ as a function of the input power ($\kappa = \Omega_m/10$). The minima correspond to the SQL of the 1RT and 3RT. (b) The measurement uncertainty at the SQL as a function of the normalized cavity lifetime. (c) The input power required to reach the SQL as a function of the cavity lifetime. For the 3RT the SQL is reached at significantly lower powers. Both insets show, that the 3RT merges with the 1RT in the limit $\kappa \gg \Omega_m$, when the resonances overlap [cf. Eq.7].

uncertainty, because it does not consider any correlation effects, i.e., \bar{S}_{x_F} , which become non-zero when $\Delta \neq 0$ or $\Theta \neq \pi/2$. For the 3RT, the SQL in the RSB is $\sqrt{3}$ times larger than that for the 1RT. As already discussed earlier, the increase of QBA and sensitivity allows to reach the SQL at lower power. The difference in the SQL arises from the fact, that the increase in QBA is three times larger than the improvement in sensitivity [cf. Fig.3]. In the limit $\kappa \gg \Omega_m$, the optical modes overlap and the 3RT becomes an effective 1RT (with modified κ , which has been considered in the power dependence of Fig.3). In this limit the SQL of the resonant 1RT is recovered [cf. Eq.7].

Furthermore, we calculate the ratio of the powers to reach the SQL in the resonant 1RT and 3RT for $\Omega = \Omega_m$: $P_{SQL}^{single}/P_{SQL}^{triple} = (1/\sqrt{3}) \cdot 4\Omega_m^2/\kappa^2$. In recent experimental realizations, this factor can easily exceed 10^2 [10, 13]. In a concrete experimental realization it is noted that the SQL anyhow only pertains to highly ideal measurements, i.e. operating overcoupled ($\eta_c = 1$) Therefore the factor of $\sqrt{3}$ is a modest penalty in most experiments, compared to the substantial reduction of power to reach the SQL that is highly advantageous in any experimental setting.

Experimental implementation.— In the present section, three possible implementations, reflecting state of the art research endeavors, are described. *First*, it is noted that the effect can be readily implemented using Fabry Perot cavities, due to the degeneracy of the higher order modes of a confocal mirror cavity [cf. Fig. 1]. Here, the experimental feasibility has recently been discussed for a Fabry Perot cavity[24] and in general has been studied in the context of the parametric instability in LIGO[23, 25, 26]. *Second*, the effect can be imple-

mented in microsphere cavities, featuring an azimuthal mode spectrum with closely spaced modes, which can be tuned by strain to match the mechanical frequencies of the spheres. *Third*, dual or triple resonances can also be implemented using superconducting coplanar waveguide resonators which can be coupled to nanomechanical beams[10]. Coupling of two (frequency degenerate) CPW resonators via a mutual coupling capacitance can lead to normal mode splitting, enabling a 2RT configuration. Using a three degenerate CPW, the mutual coupling allows realization of the 3RT scheme.

* Electronic address: tobias.kippenberg@epfl.ch

- [1] V. B. Braginsky and F. Khalili, *Quantum Measurement* (Cambridge University Press, 1992).
- [2] D. G. Blair, E. N. Ivanov, M. E. Tobar, P. J. Turner, F. van Kann, and I. S. Heng, Phys. Rev. Lett. **74**, 1908 (1995).
- [3] V. B. Braginsky, *Measurement of Weak Forces in Physics Experiments* (University of Chicago Press, 1977).
- [4] C. M. Caves, Phys. Rev. D **26**, 1817 (1982).
- [5] A. A. Clerk, M. H. Devoret, S. M. Girvin, F. Marquardt, and R. J. Schoelkopf, 0810.4729 (2008).
- [6] C. M. Caves, Phys. Rev. Lett. **45**, 75 (1980).
- [7] P. Verlot, A. Tavernarakis, T. Briant, P. F. Cohadon, and A. Heidmann, arXiv:0809.2510 (2008).
- [8] A. Naik, O. Buu, M. D. LaHaye, A. D. Armour, A. A. Clerk, M. P. Blencowe, and K. C. Schwab, Nature **443**, 193 (2006).
- [9] K. R. Brown, J. Britton, R. J. Epstein, J. Chiaverini, D. Leibfried, and D. J. Wineland, Phys. Rev. Lett. **99**, 137205 (2007).
- [10] J. D. Teufel, J. W. Harlow, C. A. Regal, and K. W. Lehnert, Phys. Rev. Lett. **101**, 197203 (2008).
- [11] T. J. Kippenberg and K. Vahala, Science **321**, 1172 (2008).
- [12] S. Gigan, H. R. Bohm, M. Paternostro, F. Blaser, G. Langer, J. B. Hertzberg, K. C. Schwab, D. Bauerle, M. Aspelmeyer, and A. Zeilinger, Nature **444**, 67 (2006).
- [13] A. Schliesser, R. Riviere, G. Anetsberger, O. Arcizet, and T. J. Kippenberg, Nature Phys. **4**, 415 (2008).
- [14] I. Wilson-Rae, N. Nooshi, W. Zwerger, and T. J. Kippenberg, Phys. Rev. Lett. **99**, 093901 (2007).
- [15] F. Marquardt, J. P. Chen, A. A. Clerk, and S. M. Girvin, Phys. Rev. Lett. **99**, 093902 (2007).
- [16] C. W. Gardiner and P. Zoller, *Quantum Noise* (Springer, 2000).
- [17] M. Jaekel and S. Reynaud, Europhysics Letters **13**, 301 (1990).
- [18] A. F. Pace, M. J. Collett, and D. F. Walls, Phys. Rev. A **47**, 3173 (1993).
- [19] S. Mancini and P. Tombesi, Phys. Rev. A **49**, 4055 (1994), part B.
- [20] M. P. Blencowe and E. Buks, Phys. Rev. B **76**, 014511 (2007).
- [21] O. Arcizet, T. Briant, A. Heidmann, and M. Pinard, Phys. Rev. A **73**, 033819 (2006).
- [22] C. Fabre, M. Pinard, S. Bourzeix, A. Heidmann, E. Giacobino, and S. Reynaud, Phys. Rev. A **49**, 1337 (1994).

- [23] W. Kells and E. D'Ambrosio, Phys. Lett. A **299**, 326 (2002).
- [24] H. Miao, C. Zhao, L. Ju, S. Gras, P. Barriga, Z. Zhang, and D. G. Blair, Phys. Rev. A **78**, 063809 (2008).
- [25] V. B. Braginsky, S. E. Strigin, and S. P. Vyatchanin, Phys. Lett. A **287**, 331 (2001).
- [26] C. Zhao, L. Ju, J. Degallaix, S. Gras, and D. G. Blair, Phys. Rev. Lett. **94**, 121102 (2005).
- [27] The bar denotes a symmetrized spectral density: $\bar{S}[\Omega] =$
- $^{1/2}(S[\Omega] + S[-\Omega])$.
- [28] Terms of the order Ω_m/ω_0 have been neglected, because they are in general very small.
- [29] This is readily done, because we do not consider a squeezed input state.
- [30] However, for the same input power, QBA in the 2RT is enhanced, compared to the 1RT_{det}, as resonant pumping increases g_m^2 by $4\Omega_m^2/\kappa^2$.